

Federated Feature Selection for Cyber-Physical Systems of Systems

Pietro Cassar, Alberto Gotta, and Lorenzo Valerio

Abstract—Autonomous systems generate a huge amount of multimodal data that are collected and processed on the Edge, in order to enable AI-based services. The collected datasets are pre-processed in order to extract informative attributes, called features, which are used to feed AI algorithms. Due to the limited computational and communication resources of some CPS, like autonomous vehicles, selecting the subset of relevant features from a dataset is of the utmost importance, in order to improve the result achieved by learning methods and to reduce computation and communication costs. Precisely, feature selection is the candidate approach, which assumes that data contain a certain number of redundant or irrelevant attributes that can be eliminated. The quality of our methods is confirmed by the promising results achieved on two different data sets. In this work, we propose, for the first time, a federated feature selection method suitable for being executed in a distributed manner. Precisely, our results show that a fleet of autonomous vehicles find a consensus on the optimal set of features that they exploit to reduce data transmission up to 99% with negligible information loss.

Index Terms—Internet of Things, Autonomous System, Human State Monitoring, Feature Selection, Machine Learning, Federated Learning, Artificial Intelligence.

I. INTRODUCTION

AUTOMATION enables a system to run with a minimum human assistance, which evolves into autonomy when the human is taken out of the sensing, decision, and actuation loop. Automation can be used to operate a Cyber Physical System of Systems (CPSoS) comprising complex, dynamic, virtual and physical resources, such as telecommunication networks, computing units, software, sensors, and machines. Humans can interact with an autonomous system either as passive end-users of the service (such as passengers in autonomous transportation system) or rather as active co-operators in a mutual empowerment relationship towards a shared goal. Such cooperative, connected and autonomous systems of systems have the potential to be a game-changer in multiple domains if they were capable of positively exploiting such an inescapable human factor. Artificial Intelligence (AI) allows components, services, applications, and their developers to abstract from the details of fast-flowing low-level data, such as sensor feeds. Adaptive AI techniques allow to learn from a past experience and to predict the effect of actions and interactions within the CPSoS, with the physical world and, ultimately, with humans. The increasing development of semi-Autonomous Driving Systems (ADSs) poses the challenge of taking the

end-user, in the middle of the evolution process toward fully ADSs.

Aside from Autonomous Vehicle (AV) control, a Cyber Physical System (CPS) needs to monitor the comfort or discomfort of the driver to improve its well-being state, increasing the degree of safety with which the vehicle is driven.

In particular, the risk perception and the reaction to external inferences may differ from person to person and this leads to the necessity of deeper customization of how an AV works. AI is already a fundamental technology for deploying the future CPSoS for autonomous applications. The stringent computational and memory requirements for AI algorithms will impose a significant rethinking of the underlying computing and communication system. Hence, an effective AI for a CPSoS should exhibit certain key design features. Machine intelligence, in automotive scenarios, is of distributed and pervasive nature, where the AI components can be potentially deployed in every element of a CPSoS, enabling to embed intelligence at the edge, close to where the information is produced by the devices or close to where the application consumes the AI predictions. Information extraction should follow as much as possible optimal criteria, cooperating with the inherently distributed nature of the system of systems. This allows containing the flooding of noisy, redundant, heterogeneous data produced by a CPSoS, with seemingly impacting reductions in communication, storage, and energy consumption costs. Local consumption of information can also be an advantage in scenarios of unreliable connectivity or when data privacy is a key issue. Reducing the time needed to transfer either raw data or features derived from them is of the utmost importance in determining the performance of computation offloading. Intuitively, traditional data compression techniques, such as JPEG for the images, could reduce such a delay component, but will also degrade the relative classification performance [?], prolonging the training phases as well as degrading the inference performance in most settings. Conversely, when information extraction algorithms produce massive streams of features, choosing the most relevant ones to feed a Machine Learning (ML) model becomes very convenient, as proved in the following of this work. Such an operation is known as Feature Selection (FS) [3] and allows for using simpler and, therefore, more efficient ML-based models [4].

In this work, we focus on a set of AVs that collect, through their sensors, multi-modal raw measurements that are pre-processed on-board to extract the features to be transferred to a remote edge server. Due to the deterministic design of the feature extraction procedure, it is almost impossible to avoid the presence of information redundancy, which leads to a waste of computing and communication resources. A way

P. Cassar and A. Gotta are with the National Research Council, Institute of Information Science and Technologies, Pisa, PI, 56124 Italy e-mail: {pietro.cassara@isti.cnr.it, alberto.gotta@isti.cnr.it}

L. Valerio is with the National Research Council, Institute of Informatics and Telematics, Pisa, PI, 56124 Italy e-mail: lorenzo.valerio@iit.cnr.it.

to contrast such a waste is selecting and transmitting only the relevant features. However, due to the local collection process performed by each AV, the selected features represent a partial subset of those that characterize the whole process and might be inconsistent to model it. Therefore, in order to keep the information content consistent among all AVs, FS should be a collaborative process, in order to exploit and combine the whole information contained in all the local datasets. We tackle this problem, by proposing, for the first time, a Federated-Feature Selection (FFS) algorithm, exploiting a distributed computing paradigm applied to AVs. In FFS all AVs collaborate to come up with the minimal set of features selected from their local data sets, before transmitting their data to the edge server. Our method is made of two components, i) a FS algorithm that processes the local data on the AVs and, ii) an aggregation algorithm executed on the Edge Server (ES) that combines the local estimates transmitted by the AVs. Note that, the proposed approach does not need to share any local data but only the estimates of the local most informative features. Moreover, it guarantees that all the AVs reach a consensus on the subset of the most informative features, after a finite number of communication rounds between the AVs and the ES. The FS algorithm based on the Mutual Information (MI) metric [5], [6], is solved using the Cross-Entropy (CE) method [7]. The benefits of using CE method are twofold. On the one hand, CE can approximate a native NP-hard problem into a convex or quasi-convex problem, as shown in the next sections. On the other hand, CE is suitable for designing both centralized and distributed algorithms. The aggregation algorithm is based on a Bayesian approach through which we merge the information sent by the AVs to the ES. We rely on a Bayesian approach, where the information shared by AVs are probability vectors where each element is the estimated probability to select that feature. As we will show in the paper, this design choice reduces the control traffic generated during the distributed feature selection process.

The proposed algorithm provably converges to a subset of features which effectively compresses the data collected by the AVs. Specifically, numerical results show that, on reference benchmarks, our solution compresses data up to 99% at no significant degradation of their informative content, i.e., a learning model trained on the selected features is as accurate as a model trained on the whole feature set.

Summarising, the novel contributions of this paper are:

- A novel FFS algorithm based on CE (client-side) and a Bayesian aggregation approach (server-side).
- The theoretical proof that our distributed algorithm converges to a solution in a fixed number of iterations.
- An extended numerical evaluation on two real-world datasets showing the compression performance of our solution.

The paper is organized as follows: related works are presented in Section II; the reference scenario and the system assumptions are presented in Section III; the theoretical background underlying the proposed feature selection approach is presented in Section IV; the federated version of the feature selection algorithm is presented in Section V; the Section VI

presents the experimental results of a study case with two real world datasets, belonging to different application domains; finally the Conclusions in Section VII.

II. RELATED WORKS

A. Feature Selection

Many FS procedures have been proposed in the literature. In [3], [8], [9] authors provide a comprehensive overview of the existing methods. Additionally, they consider the most important application domains and review comparative studies on feature selection therein, in order to investigate, which methods outperform for specific tasks. Authors highlight that FS is based on the identification of the relevance and redundancy provided by the features with respect to a class attribute function. The main approaches of FS fall into three categories: filtering, wrapping, and embedded methods. This categorisation is based on the interaction between the selected features and the learning model adopted to take a decision. The output of the wrapping and embedded methods is tightly connected to the learning model that uses the selection. Therefore, with these methods the feature selection and the model training cannot be uncoupled. Conversely, filtering methods are suitable for being used regardless the presence of a learning model to train. As shown in [3], [8], [9], most of the well-known filtering algorithms use information-based metrics for FS, and can deal with samples of variable lengths, as presented in [10], [11]. A suitable information-based metric for the FS is the MI. MI has gained increasing popularity in data mining, for its ease to use, effectiveness, and strong theoretical foundation. However, the formulation of the underlying optimization problem is NP-Hard [5], [6], i.e., MI-based feature selection problem involves the integer programming or in some cases the quadratic integer programming. In [12]–[14] authors show how to adopt the CE approach to address such native computational complex problems, for different application scenarios. To the best of our knowledge, all these algorithms are designed for being executed in a centralised setting, i.e., under the assumption that the whole dataset is available to the algorithm, without limitations.

B. Distributed Learning

Distributed learning, in the literature, is considered from several perspectives. A very consistent body of work deals with distributed learning based on the Federated Learning (FL) framework. FL is a distributed learning framework initially proposed by Google, where a large number of mobile or edge devices participate in a collective and distributed training of a shared model. [15], [16]. Federated Learning is an iterative procedure spanning over several communication rounds until the convergence is reached. Based on this paradigm, several modifications have been proposed concerning (i) new distributed optimisation algorithms [17]–[20], and (ii) privacy-preserving methods for federated learning [21], [22]. Alternatively, other approaches do not rely on a centralised coordinating server. In [23], [24], authors propose a distributed and decentralised learning approach based on Hypothesis Transfer Learning (HTL). Similarly to the Federated Learning

framework, authors assume that several devices hold a portion of a dataset to be analysed by some distributed machine learning algorithms. The aim of [23], [24] is to provide a learning procedure able to train, in a decentralised way, an accurate model while limiting the network traffic generated by the learning process. The vast majority of the distributed learning solutions, presented in the literature, focus on the model's training, giving the feature engineering phase for granted. Until now, the idea of performing FS, directly, on edge devices remains unexplored.

In the literature only few approaches that cope with FS in distributed settings. In [25], authors present a distributed algorithm for the feature selection based on the Intermediate Representation. The purpose of the Intermediate Representation is to preserve the privacy of data that allow the node to exchange to each other the data they hold. Therefore, in this method tFS is performed under the assumption that all data are available to the FS algorithm. Moreover, the method presented by the author depends from the specific learning model that uses the selected features.

To the best of our knowledge, this is the first paper that proposes a federated mechanism of feature selection explicitly designed to meet the requirements of the CPSoS context.

III. SYSTEM ASSUMPTIONS

In this section we describe the reference scenario and the system assumptions considered in this paper, as shown in Figure 1. We consider a scenario where a set of AVs, implementing an ADS each, collect data generated by the sensors integrated in a CPSoS and collaborate with the others ADSs to learn the minimal, and most informative, set of features from their local dataset. To this end, AVs execute an in-network data filtering process through our FFS approach. In this phase, AVs exchange with each others control information in order to reach a consensus to identify the most informative feature set. Finally, the globally shared feature set is use as compression scheme before starting the transmission of data to the ES. Note that, in this system the AVs are only responsible for finding, in a collaborative way, the best compression scheme applicable to the their local data, based only on the control information they exchange with each others. Moreover, the ES has a three-fold role: i) it act as central coordinating entity in the FFS process whose purpose is to aggregate the partial control information sent by the AVs; ii) it acts as final collector for the compressed data, once the FFS is completed and, iii) runs the AI algorithm to extract knowledge from data.

To validate the performance of the proposed FFS method we target two different user cases. The first one refers to the localization of an AV in the environment based on images and inertial measurements, and the second one regards the physiological-state monitoring in the automotive domain. We define two different sub-systems part of the same CPSoS: the ADS of above, and an Human State Monitoring System (HSMS) to learn the feeling perceived from a passenger relatively to the ADS driving style. Therefore, we assume each AV to be equipped with a camera to capture images from the surrounding environment aside some inertial sensors,

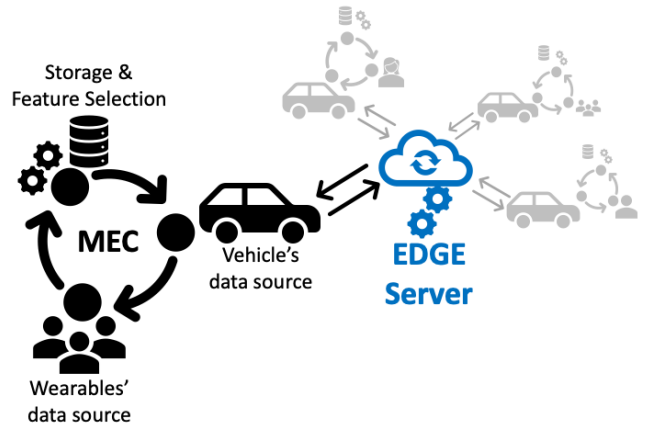


Fig. 1: System architecture. Data sources characterize two different CPSs: the former that monitors the user through wearable sensors, the latter relative to the ADS.

for the former learning task, and a set of body sensors, such as, Electrocardiography (ECG), Electrodermal Activity (EDA), Electromyography (EMG), and Respiration (RSP) for the latter task. Each AV is able to locally synchronize the multi-sensory data such that, for each image, it is possible to associate the corresponding inertial measurements leading to an *enhanced Raw Input Datum* (eRID). Moreover, we assume that, according to the scenario at hand, each AV is able to associate a label to the collected data, e.g., a GPS location, relative positioning, or a feedback by the user, or any other information that can be added to the data and used only for training the ML model. Note that for the scope of this paper it is not important the specific semantic of the labelling, but it is enough to assume a labelling process. AVs are also equipped with a relatively small edge computing unit (e.g., a RaspberryPi or, at most, an Nvidia Jetson Nano) able to cache data and executing the feature selection task, before starting the data transmission. Additionally, AVs are endowed with a radio communication interface to communicate toward the ES. It must be noted that the task is not collecting images of the environment, or physiological parameters of the user but, conversely, retrieving the information associated to those images or to those physiological sensors, e.g., the position of the AV with respect to the surrounding or the user mood. In particular, the latter is labelled according to the classification scale provided by questionnaires like PANAS, SSSQ or SAM [26], which associates numerical labels to the physiological states.

IV. FEATURE SELECTION

In this section, we provide the theoretical background of the MI-based feature selection problem and its algorithmic solution based on the CE method.

A. Background knowledge on Mutual Information

The FS problem can be formally stated as follows:

Definition (FS Problem). *Given the input data matrix \mathbf{X} composed by n samples of m features ($\mathbf{X} \in \mathbb{R}^{n \times m}$), and*

the target attributes' (or labels) vector $\mathbf{y} \in \mathbb{R}^n$, the feature selection problem is to find a k -dimensional subset $\mathbf{K} \subseteq \mathbf{X}$ with $k \leq m$, by which we can characterize \mathbf{y} .

Now let's start providing the necessary background knowledge on MI that we use to measure the amount of information obtained about the class attribute through the set of selected features. The MI between random variables \mathbf{A} and \mathbf{B} is symmetric and non-negative, and it is strictly related to the entropy $\mathbf{H}(\cdot)$, which defines the amount of information held by the variables. The entropy $\mathbf{H}(\mathbf{A})$ increases if the probability of \mathbf{A} 's is small, otherwise the entropy decreases. Hence, we can assert that the entropy measures the diversity of \mathbf{A} in terms of the uncertainty of its outcomes. MI between random variables can be defined as [28], [29]:

$$\mathbf{I}(\mathbf{U}; \mathbf{y}) = \mathbf{H}(\mathbf{y}) - \mathbf{H}(\mathbf{y}|\mathbf{U}), \quad (1)$$

where $\mathbf{U} = \{\mathbf{x}_1 \cdots \mathbf{x}_k \mid k \leq m\} \subseteq \mathbf{X}$, and $\mathbf{H}(\mathbf{y}|\mathbf{U})$ is the conditional entropy which measures the amount of information needed to describe \mathbf{y} , conditioned by the information carried by \mathbf{U} . Hence, $\mathbf{I}(\mathbf{U}; \mathbf{y})$ represents the dependence between \mathbf{U} and \mathbf{y} , i.e., the greatest is the value \mathbf{I} , the greatest is the information carried by \mathbf{U} on \mathbf{y} . The features selected in \mathbf{U} are Essential Attributes (EAs), also known as Markov Blanket [5], [27]. So, if the features in \mathbf{U} are EAs, then the equation (1) gets its maximum. The above considerations, and the Theorem 1 stated in the following provide the basis to develop our FS algorithm, whose rigorous proof is addressed in [28], [29].

Theorem 1. *If the MI between \mathbf{U} and \mathbf{y} is equal to the entropy of \mathbf{y} , then \mathbf{y} is function of \mathbf{U} .*

In Equation (2) we define the optimization problem that, if solved it would provide the optimal global solution for the FS problem.

$$\arg \max_{\mathbf{U}} \mathbf{I}(\mathbf{U}; \mathbf{y}) \quad (2)$$

$$\mathbf{U} = \{\mathbf{x}_1 \cdots \mathbf{x}_k \mid k \leq m\} \subseteq \mathbf{X}$$

Since the optimal solution \mathbf{U} is found among all combinations of feature indices of the native set \mathbf{X} , this is an Integer Programming (IP) optimization problem that is NP-hard [30].

A way to make it computationally tractable, is to approach it through an iterative algorithm which selects and adds to the subset \mathbf{U} one feature at a time as defined in Equation 3

$$\arg \max_{\mathbf{x}_j \in \mathbf{X} \setminus \mathbf{U}} \mathbf{I}(\mathbf{x}_j; \mathbf{y}|\mathbf{U}), \quad (3)$$

$$\mathbf{U} = \{\mathbf{x}_1 \cdots \mathbf{x}_{k-1} \mid k \leq m\} \subseteq \mathbf{X}.$$

The main drawback of this algorithm is the it might end up with a sub-optimal solution because selecting the features one by one the algorithm makes the implicit assumption that they are independent, which might not hold true. Theoretical foundations for the incremental version of the feature selection algorithms has been proven by the authors in [28], [29]

Another issue in dealing with the optimization problem in (2)-(3) is how efficiently evaluating both the entropy and MI even for datasets with a small number of samples. This

problem can be overcome, by using the powerful numerical tool MIToolbox [27].

Before dealing with a numerically tractable solution of the problem in equations (2)-(3), we want to provide an intuitive proof based on the relation between MI and the entropy. Considering the example in Figure 2, the circles are the entropy of the random variables $\mathbf{A}, \mathbf{B}, \mathbf{U}, \mathbf{y}$, and the gray regions are the information carried by the variable $\mathbf{A}(\mathbf{B})$ on \mathbf{y} . The dashed area shows the information redundancy of the variable $\mathbf{A}(\mathbf{B})$ given the already selected variables in \mathbf{U}_{j-1} . In this example, the variable \mathbf{A} is the one that should be added to the set \mathbf{U} because it is more informative than \mathbf{B} on \mathbf{y} , i.e., its grey area is larger than the one of \mathbf{B} , and it is less redundant than \mathbf{B} w.r.t. to \mathbf{U}_{j-1} .

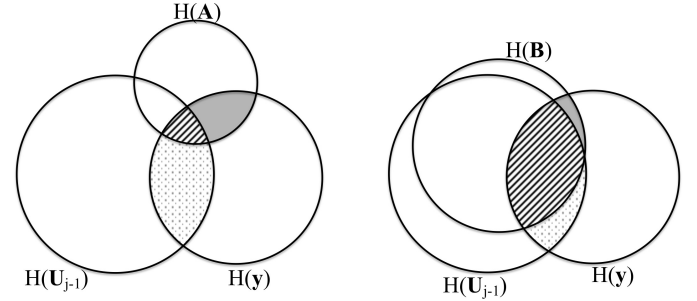


Fig. 2: Example of the relationship between Mutual Information and Entropy

B. CE-based feature selection based algorithm

In this section, we provide an algorithm that in a finite number of steps is able to find a solution that well approximates that found by solving Problem (2) making negligible the assumption of independence among features introduced in Problem (3). This means that, instead of selecting one EA at a time, we can select a set of EAs jointly.

Our algorithm is based on the following condition: if the set \mathbf{U} contains only EAs, then $\mathbf{I}(\mathbf{U}; \mathbf{y}) \rightarrow \mathbf{H}(\mathbf{y})$, which implies that $\mathbf{H}(\mathbf{y}|\mathbf{U}) \rightarrow 0$ [28], [29]. Note that with our approach, we avoid the greedy research of the set \mathbf{U} , among all the possible $\binom{m}{k}$ solutions, which realizes $\mathbf{H}(\mathbf{y}|\mathbf{U}) \rightarrow 0$. To this end, we adopt the stochastic research of the solution. The idea behind the proposed approach is to associate the i -th feature, with $i = 1, \dots, m$, to a binary variable $z_i \sim \text{Bernoulli}(p_i)$. Our algorithm finds the variables $z_i, i = 1, \dots, m$ that must have $p_i \rightarrow 1$, so that the objective function $\mathcal{O}(\mathbf{U}(\mathbf{z}))$ given by $\mathbf{H}(\mathbf{y}|\mathbf{U})$ is close to 0. This is called Associated Stochastic Problem (ASP) [7]. In this way, we get the optimal distribution of the binary vector \mathbf{z} through which we identify the features to select, i.e. the i -th feature is selected if $p_i \rightarrow 1$. It is worth noting that searching the solution of the optimization problem through the definition of the ASP has the advantage to address the native problem in equations (2) as convex problem.¹

We can formulate the ASP as a minimization problem, as shown in the following. Briefly, we need to find the probability

¹More details are in Section 4 of [7].

distribution $g(\mathbf{z}, \mathbf{p})$ of the values in \mathbf{z} equal to 1 that solves the equation:

$$P_{\mathbf{p}}(\mathcal{O}(\mathbf{U}(\mathbf{z})) \leq \gamma) = \sum_{\{\mathbf{z}\}} \mathcal{I}_{\{\mathcal{O}(\mathbf{U}(\mathbf{z})) \leq \gamma\}} g(\mathbf{z}, \mathbf{p}) \quad (4)$$

where $\mathcal{I}_{\{\cdot\}}$ is the indicator function of the event $\mathcal{O}(\mathbf{U}(\mathbf{z})) \leq \gamma$, and γ is the minimum value for our objective function. Precisely, γ at step t is calculated as the percentile $1 - \beta$ of the objective function calculated using the samples drawn from the distribution $g(\mathbf{z}, \mathbf{p})$ at step t . Note that, the authors in [7] recommend to set β in the range $0.9 - 0.95$

The indicator function is equal to 1 for all the possible configurations in \mathbf{z} that verify the event $\mathcal{O}(\mathbf{U}(\mathbf{z})) \leq \gamma$, and 0 otherwise.

A well known approach to estimate $g(\mathbf{z}, \mathbf{p})$ is to use the Likelihood Ratio (LR) estimator with reference parameter \mathbf{p} . The optimal value \mathbf{p}^* for the distribution can be calculated from the theory of LR estimation [7] through the following equation:

$$\mathbf{p}^* = \arg \min_{\mathbf{p}} \frac{1}{S} \sum_{j=1}^S \mathcal{I}_{\{\mathcal{O}(\mathbf{U}(\mathbf{z}_j)) \leq \gamma\}} \ln(g(\mathbf{z}_j, \mathbf{p})) \quad (5)$$

where $\mathbf{Z} = \{\mathbf{z}_1, \dots, \mathbf{z}_S\}$ is a set of possible samples drawn from the distribution $g(\mathbf{z}, \mathbf{p})$.

As stated above $\mathbf{z}_j = [z_{1j} \dots z_{mj}]$ is a vector of independent Bernoulli random variables where z_{ij} takes value equal to 1 with probability p_i and 0 with probability $1 - p_i$. Hence, $g(\mathbf{z}_j, \mathbf{p})$ can be written as:

$$g(\mathbf{z}_j, \mathbf{p}) = \prod_{i=1}^m p_i^{z_{ij}} (1 - p_i)^{(1-z_{ij})}; z_{ij} \in \{0, 1\} \quad (6)$$

Given that objective function in equation (5) is concave ², a closed form for the solution can be found by imposing:

$$\frac{\partial}{\partial p_i} \frac{1}{S} \sum_{j=1}^S \mathcal{I}_{\{\mathcal{O}(\mathbf{U}(\mathbf{z}_j)) \leq \gamma\}} \ln(g(\mathbf{z}_j, \mathbf{p})) = 0,$$

leading to:

$$p_i = \frac{\sum_{j=1}^S \mathcal{I}_{\{\mathcal{O}(\mathbf{U}(\mathbf{z}_j)) \leq \gamma\}} z_{ij}}{\sum_{j=1}^S \mathcal{I}_{\{\mathcal{O}(\mathbf{U}(\mathbf{z}_j)) \leq \gamma\}}} \quad i = 1 \dots m; \quad (7)$$

In the practical use, the result in the equation (7) is used for updating the distribution \mathbf{p} as follows:

$$p_i = (1 - \alpha)p_i + \alpha \frac{\sum_{j=1}^S \mathcal{I}_{\{\mathcal{O}(\mathbf{U}(\mathbf{z}_j)) \leq \gamma\}} z_{ij}}{\sum_{j=1}^S \mathcal{I}_{\{\mathcal{O}(\mathbf{U}(\mathbf{z}_j)) \leq \gamma\}}} \quad (8)$$

The mathematical analysis about the choice of the parameter α is provided in the Appendix of this work. Further, indications on the choice of α can be found in [7], [33]. The derivation of equations (5-7), as well as, the optimality of $g(\mathbf{z}_j, \mathbf{p})$ is proven in [7].

The solution of the problem defined in (5) is achieved through Algorithm 1.

²The logarithm is a concave function, the indicator function is 0 or 1 so the weighted sum of concave functions gives still a concave function.

Algorithm 1 CE-based algorithm for FS

```

1: procedure CE( $\mathbf{X}, \mathbf{y}, \mathbf{p}^G$ )
2:    $\mathbf{p}^l \leftarrow \mathbf{p}^G$ 
3:    $\mathbf{Z} \leftarrow \text{generateRandomSample}(S, \mathbf{p}^l)$ 
4:    $\mathbf{u} \leftarrow \{\}$ 
5:   for all  $\mathbf{z} \in \mathbf{Z}$  do
6:      $\mathbf{U} \leftarrow \text{getSubset}(\mathbf{X}, \mathbf{z})$ 
7:      $\mathbf{u} \leftarrow \mathbf{u} \cup \mathbf{H}(\mathbf{y}|\mathbf{U})$ 
8:   end for
9:    $\gamma \leftarrow \text{computePercentile}(\mathbf{u}, 1 - \beta)$ 
10:   $\text{updateProbabilities}(\mathbf{p}^l, \mathbf{u}, \gamma)$  ▷ Eq. (8)
11:  return  $\mathbf{p}^l$ 
12: end procedure

```

V. FEDERATED FEATURE SELECTION

In this section we present how we exploit the cross-entropy based feature selection algorithm presented in Section IV and summarised in Algorithm 1 to design our distributed and federated feature selection algorithm FFS, described in Algorithms 2 and 3. They cover, respectively, the two functional blocks of FFS, i.e., Algorithm 2 is executed by the ES to coordinate the distributed feature selection and Algorithm 3 runs on the clients. The FFS is an iterative procedure. In the beginning, the ES sends to the clients involved in the process a vector $\mathbf{p}^G \in \mathbb{R}^d$ where each element represents the probability that each feature has to be selected according to its importance (lines 8-10 of Alg.2). Each element of \mathbf{p}^G is initialized to 0.5, i.e., this is a common choice when using the CE algorithm. The vector \mathbf{p}^G represents a piece of global information that the ES shares with the client nodes. Each client l uses it to initialize its local copy of the probability vector \mathbf{p}^l and runs the local feature selection procedure based on its local data (lines 2-3 of Alg. 3). At the end of the local feature selection, the l -th client sends to the ES the locally updated features' probability vector $\mathbf{p}_{\text{new}}^l$ and a control information regarding the cardinality of its local data n^l whose purpose will become clear in the following. The ES computes the new global probability vector by aggregating the ones received from the clients (line 13 of Alg. 2). The updated vector \mathbf{p}_{r+1}^G is transmitted to the nodes that, once received, they run Algorithm 3 initializing the local probability vector with the new global one. This procedure iterates until the distribution global probability vector converges to a stable one. In FFS we check convergence by comparing the distribution of the current global probability vector \mathbf{p}_r^G to the previous one \mathbf{p}_{old}^G using the Kolmogov-Smirnov statistical test for two one-dimensional samples (KS-test). The procedure stops when (i) the p-value of the KS-test is greater than a fixed threshold ($\tau_1 = 0.995$)³ and, (ii) its variation from one update to the other is negligible, i.e., $\tau_2 = 10^{-6}$ (line 7 of Alg. 2).

The core point of Algorithm 2 regards the aggregation step (line 13 al Alg. 2) where the ES merges the local probability vectors into the global one, which, in our solution it is defined as a weighted average. Formally, we assume that each node

³We empirically observed that the closer τ_1 to one, the more accurate the solution.

acquires a number of *i.i.d.* records n^l to perform FS, and that the nodes share the same set of features \mathbf{X} . The global probability \mathbf{p}^G used for the FS can be written as follows:

$$\mathbf{p}^G = \sum_l \mathbf{p}^l q^l, \quad (9)$$

where $\mathbf{p}^{(l)}$ is the solution of problem (5) at node l obtained using Algorithm 1, and $q^{(l)}$, whose formal definition is provided in equation (10) weights the probability vector of node l w.r.t. the other nodes.

$$q^l = \frac{n^l}{\sum_l n^l} \quad (10)$$

According to equation (10), we weight the probability vector p^l of node l proportionally to the size of its local dataset compared to the whole amount of data present in the system. In this way, we can contrast situations where local datasets are heterogeneous w.r.t. the size.

In FFS, the updating scheme can be, at least in principle, both synchronous and asynchronous, provided that the set of nodes involved in the process does not change over time.⁴ Precisely, we assume a system where the ES expects, after sending the updated global probability vector to the nodes, to receive their local updates within a fixed time slot, after which, it begins the aggregation step using only the information received. Therefore, the number of updates' used to compute the new global probability vector might change because a subset of nodes could not communicate their update within the time limit imposed by the ES. Regardless of the number of nodes that contributed to the aggregation step during one round of communication, the ES broadcasts the new global probability vector \mathbf{p}^G to *all* nodes in the system. In this way, all nodes start the new round of local computation from the same starting point, and, consequently, we dramatically limit the potentially detrimental effects deriving from the aggregation of outdated local probability vectors. Moreover, as proved by the convergence analysis provided in the Appendix, independently from the updating scheme, FFS converges the infinite number of steps to the very same solution that would be found running the CE-based algorithm for FS in centralised settings i.e., with complete access to the entire dataset.

VI. NUMERICAL EVALUATION

In this section, we present the numerical results of our compression method based on the FFSn algorithm presented in Section V. Before going through the results, we introduce the datasets, the simulation settings, the methodology, and the metrics used to evaluate our solution's performance.

A. Dataset description and simulation settings

We based the performance evaluation of FFS on two datasets, each one mapping one of the two use cases described

⁴Note that this condition does not imply that all nodes must be active during the entire process. In fact, as we will show in Section VI our system is robust to the presence of churning nodes.

Algorithm 2 Server side Federated Feature Selection algorithm

```

1: procedure SERVER-NODE
2:    $v \leftarrow 0$             $\triangleright$  p-value of Kolmogorov-Smirnov test
3:    $\tau_1 \leftarrow .995$ 
4:    $\tau_2 \leftarrow 10^{-6}$     $\triangleright$  Thresholds to check convergence
5:    $r \leftarrow 0$             $\triangleright$   $r$ -th communication round
6:    $\mathbf{p}_r^G \leftarrow \{1/2 \mid \forall p_i \ i = 1, \dots, m\}$ 
7:   while  $v \geq \tau_1 \wedge |v - v_{old}| \leq \tau_2$  do    $\triangleright$  repeat until
convergence is met
8:     for all  $l \in L$  do
9:       sendUpdateToClient( $l, \mathbf{p}_r^G$ )
10:    end for
11:    receiveLocalUpdateFromNodes( $\mathbf{p}_{new}^{(l)}, n^{(l)}$ )
12:     $\mathbf{p}_{old}^G \leftarrow \mathbf{p}_r^G$ 
13:     $\mathbf{p}_r^G \leftarrow$  updateGlobalProbability()    $\triangleright$  Eq. (9)
14:     $v_{old} \leftarrow v$ 
15:     $v \leftarrow$  KolmogorovSmirnovTest( $\mathbf{p}_{old}^G, \mathbf{p}_r^G$ )
16:     $r \leftarrow r + 1$ 
17:  end while
18: end procedure

```

Algorithm 3 Client side Federated Feature Selection algorithm

```

1: procedure CLIENT-NODE
2:    $\mathbf{p}^l \leftarrow$  receiveFromServer( $\mathbf{p}_r^G$ )
3:    $\mathbf{p}_{new}^l \leftarrow$  CE( $\mathbf{X}^l, \mathbf{y}^l, \mathbf{p}^l$ )    $\triangleright$  Algorithm 1
4:   sendToServer( $\mathbf{p}_{new}^l, n^l$ )
5: end procedure

```

in Section III. The first one called MAV⁵ is a publicly available dataset containing both 64×64 images and 6 Inertial Measurement Units (IMUs) collected by a AV during a mission in a controlled environment. The second dataset called WEearable Stress and Affect Detection (WESAD) is a collection of data sampled from heterogeneous biophysical sensors: ECG, EDA, EMG, Temperature, Respiration and Inertial Measurements on the three axes.

a) *MAV dataset*: In the MAV dataset, both images and inertial measurements are synchronised to obtain a set of eRIDs. Note that we pre-process the raw images to extract from them more informative features as it is customary in the computer vision domain. In our case, feature extraction eases the training of a machine learning model and, in this case, performs a preliminary step of data compression. In details, a raw image is made of 4102 floats (64×64 pixels + 6 IMU readings) while, after the feature extraction, it shrinks down to a vector of size 2166 floats. In our settings, we extract the Histogram of Oriented Gradient (HOG) features⁶, and we assume that the feature extraction is accomplished directly on the AV, which might be possible if equipped with a board of the kind discussed in [31]. Note that since the dataset does not contains labels associated with the eRIDs

⁵dataset available at: <https://tinyurl.com/mavmr01>

⁶HOG is a standard feature extraction methodology used in computer vision and image processing to create an image descriptor that captures the spatial relations between different portions of it [31].

we labelled it, in a way compatible with the original context of positioning. To this end, we associated with each eRID a label corresponding to the corresponding voxel.⁷ Table I shows the structure of an eRID for the MAV; the first 2160 features are HOG while the last 6 are IMUs, i.e., acceleration (ACC) and angular velocity (AV). The whole dataset contains 2911

TABLE I: Structure of a MAV eRID

0	1	2	...	2158	...
HOG #					
2160	2161	2162	2163	2164	2165
ACC _x	ACC _y	ACC _z	AV _x	AV _y	AV _z

labelled records. To simulate the federated data collection, we split it into ten disjoint partitions of size 291 records such that each partition is i.i.d. w.r.t. the entire dataset. Each subset represents a AV. The data collection is slotted; thus, the AVs draw with replacement a random sample from their local dataset for each slot. This sample is used to perform the local computation of the distributed algorithm followed by a communication round for synchronising the AVs on the local feature selection. Each random draw's size is accumulated to trace the cache necessary for storing data until the completion of the distributed feature selection.

b) *WESAD dataset.*: The WESAD dataset provides data in terms of features and labels already useful to perform the detection of stress and affection state of human subjects. The dataset contains readings from two devices, i.e., Respiban and Empatica E4, positioned i) on the chest and ii) on the wrist of human subjects. Each device is equipped with multiple sensors monitoring several physiological parameters. Since the two devices have different operating settings, we focused on the Respiban, whose collection rate is homogeneous for all its sensors. The dataset contains readings collected from 17 human subjects, which perform a predetermined protocol to induce the body in one of the following states: 0-baseline, 1-amusement, 2-stress, 3-meditation, 4-recovery. The data collected for each subject amounts to ~ 3.6 M records, equivalent to ~ 220 MB. A complete description of the dataset is provided in [26]. Table II shows the structure of an eRID for the WESAD. Due to the

TABLE II: Structure of a WESAD eRID

0	1	2	3	4	5	6	7
ACC _x	ACC _y	ACC _z	ECG	EMG	EDA	TEMP.	RSP

huge size of the dataset we used the data of a subset of 5 out of 17 subjects, corresponding to ~ 1.1 GB. For this dataset, data is already partitioned according the subject ID, thus we keep the original partitions. Therefore, in our simulated scenario, each partition corresponds to an edge device holding the data of only one subject, i.e., no artificial data re-distribution is performed. As for the previous scenario, each device executes the federated feature selection using only its own data and shares their estimate of the important features with the other devices as in Algorithms 2, and 3.

⁷A voxel represents a value on a regular grid in three-dimensional space.

We evaluate the performance of our methodology according to two metrics:

- *accuracy*: to assess the quality of the distributed feature selection
- *network overhead* (N_{OH}): to evaluate the impact in terms of network traffic generated by our methodology

Our target is to compress the data to be transmitted, without significantly degrading its informative content.

Accuracy metric: The quality assessment is a two-stage procedure. First, we set the baseline validating the quality of the features selected by CE executed in Centralised settings, i.e., we train a classifier using the set of selected features (CFS) on the entire dataset, and we compare its prediction performance with those of a second classifier trained on the whole set of features (NO-FS). If the CFS performance on a smaller group of features is comparable or equivalent with the one identified by NO-FS, we consider the features selection valid. Then, we repeat the same procedure training another classifier on the subset of features obtained from our methodology (FFS) and comparing its performance with CFS. We are interested in evaluating the quality of the distributed feature selection against the centralised one. We split the dataset in train (80%) and test set (20%). The train set is used for both feature selection and model training, while the test is used for performance evaluation only. The accuracy is defined as the average of correctly classified records

$$A = \frac{1}{N} \sum_{i=1}^N I(\hat{y}_i = y_i), \quad (11)$$

where N is the size of the test set, I is the indicator function, \hat{y}_i and y_i are the i -th predicted and true label, respectively. For the sake of statistical significance, the training is repeated ten times, changing the initialisation of the classifier and the composition of training and test set. The reported results are average values accompanied by confidence intervals (C.I.) at 95% of confidence.

Network Overhead: We measure the network traffic generated by our solution as follows. On the one hand, we compute the network overhead generated by the FFS network defined as:

$$N_{OH} = R * L * 2 * (z + 1 + b) \quad (12)$$

where R is the number of communication rounds before the all the L AV's involved in the distributed feature selection converge to a solution, $z + 1$ is the number of nonzero floating point numbers belonging to the probability vector \mathbf{p}^l (Eq. (9) exchanged between the AVs during each round plus the weight $p(l)$ (Eq. (10)). The symbol b is the size of the bit map used to reconstruct the position of the non-zero elements exchanged between the AVs and the edge server. On the other hand we compute the compression obtained through the feature selection as

$$C = |F|/|D| \quad (13)$$

where $F \subseteq D$ is the set of selected features and D is the entire set of features.

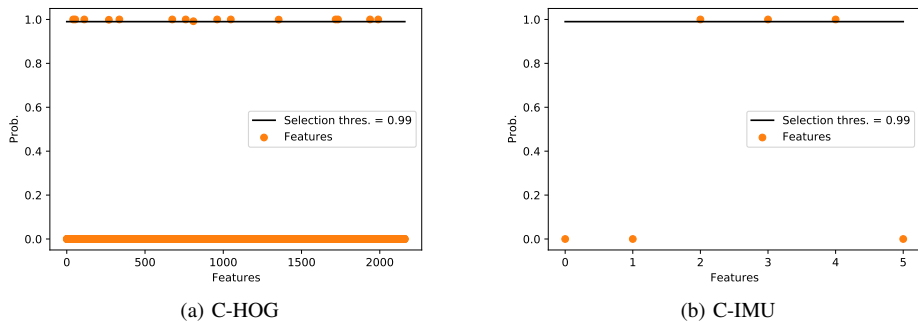


Fig. 3: Centralised Feature selection probability for HOG and IMU. The selected features are those with probability greater than 0.99 (above threshold).

B. Settings the baseline: CE in centralised settings

Let us now present the results regarding the first stage of the validation, i.e., the accuracy performance of a classifier trained using only the subset of features identified by the CE algorithm w.r.t the performance obtained by a classifier trained on the entire dataset. For this stage of validation, we train a Neural Network (NN). For MAV the NN is a multi-layer perceptron with two hidden layers of 300 and 100 neurons each. For WESAD, we used a deep NN with four hidden layers of 300,100,64,32 neurons each. The input layer’s size depends on the number of features selected, while the size output layer is 37 and 5 for MAV and WESAD, respectively. For both models the activation function is “ReLU”⁸ and the optimizer is “Adam”⁹. These are very common settings which typically provides good performance [32].

TABLE III: Comparison between NO-FS and CFS on MAV and WESAD dataset.

Dataset	Method	Size (# record)	FS (#)	C (%)	Accuracy (%)
MAV	NO-FS	2911	2166 (All)	-	0.97.5±0.4
	CFS	2911	18	99	0.96.7±0.5
WESAD	NO-FS	15*10 ⁶	8 (All)	-	94.3 ± 0.7
	CFS	15*10 ⁶	4	50	93.6 ± 0.8

Results in Table III show that CE algorithm executed on both datasets in centralised settings can identify a minimal set of features (i.e., 18 for MAV and 4 for WESAD) with the very same informative content of the whole feature set. The accuracy performance obtained by both the NN models trained on the CE’s features selection is statistically equivalent to the one obtained on the whole set of features, inducing a quite impressive compression rate (C): up to 99% and 50% of network traffic for MAV and WESAD, respectively. Finally, these results assess the suitability of the CE algorithm on both datasets, thus we can use them as benchmark for the evaluation of our distributed and federated feature selection method.

⁸Rectified Linear Unit

⁹Stochastic Gradient Descent with ADaptive Momentum

C. Evaluation of Federated Feature Selection

We focus now on the analysis of our FFS method. We compare its performance to those obtained by CE executed in centralised settings (CFS). We recall that, in federated and distributed settings, each AV can process only the data it locally collects.

First we assess the performance of FFS in a static distributed scenario where the AVs have collected all the data and, before sending it to the edge server, they perform the distributed feature selection in order to transmit only the very necessary information.

Dataset	Method	Size (# obs.)	FS (#)	C (%)	Accuracy (%±C.I.)
MAV	CFS	2911	18	99	96.7±0.5
	FFS	291	24	99	96.7±0.4
WESAD	CFS	15M	4	50	93.6±0.8
	FFS	3M	4	50	93.6±0.8

TABLE IV: Comparison between CFS and FFS on MAV and WESAD.

Table IV reveals that for MAV dataset, FFS finds a set of features that, although slightly larger than the one found by CFS (24 instead of 18), has the very same informative content, i.e., the accuracy of the NN model trained on both subsets of features are statistically equivalent. As we can see, the results also hold for the WESAD dataset. Precisely, FFS selects the same number of features identified by CFS. Specifically, FFS and CFS select the same set, i.e., the features with indexes [1,2,5,6], explaining why the NN achieves the same prediction accuracy. We motivate such an exact correspondence between FFS and CFS selection considering that the small size of the complete feature set of WESAD might prevent a high number of feature subset with equivalent informative content. Such an assumption also holds for the MAV dataset. In fact, as we can see in Figures 4a, 3b FFS and CFS select the same subset of IMU features. Conversely, when the set of features is more redundant, as it is for the HOG one, there might exist several subsets holding the same informative content. The comparison

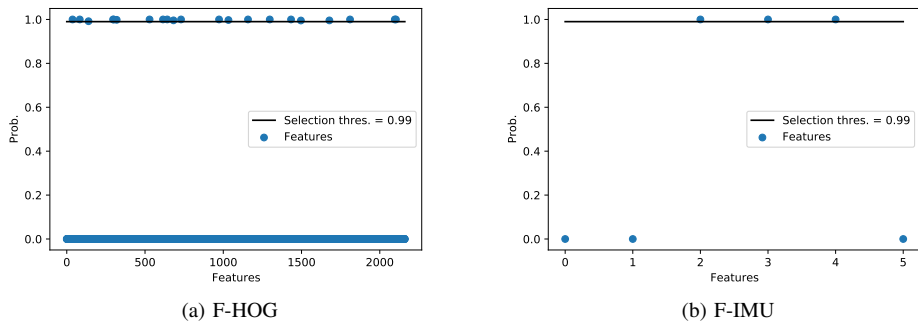


Fig. 4: Federated Feature selection probability for HOG and IMU. The selected features are those with probability greater than 0.99 (above threshold).

of Figures 4a and 3a confirms such a claim because the two feature sets are overlapping but not equal, yet the overall accuracy is comparable.

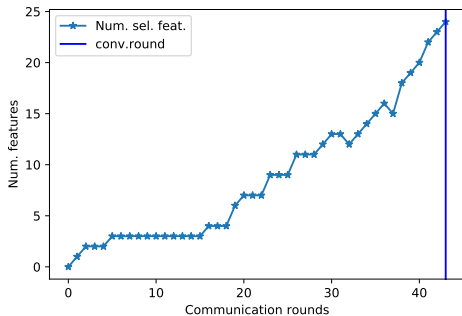


Fig. 5: Federated feature selection process on MAV dataset.

This result provides a preliminary insight regarding the effectiveness of the Bayesian aggregation used to merge the information extracted by AVs from their local datasets. Precisely, Figure 5 shows, for the MAV case, the number of selected features at each communication round. As we can see, in the beginning, the cardinality of feature selection remains almost constant. In this phase, due to the partitioning of data in separated and federated datasets, the CE algorithm has not yet enough knowledge to identify the most informative features. However, a few rounds (16), the number of features added to the selection starts increasing following an almost-linear trend. The process ends after 44 communication rounds, i.e. when the distribution of probabilities indicating the most informative features becomes stable.

Our method's capability to converge quickly to the final and most informative set of features directly affects the amount of network traffic generated upon the completion of the federated feature selection. To confirm such a claim, we performed a set of simulation in which we run FFS varying the size of the local dataset available at the edge device. In this way, we want to analyse our method's robustness when each edge device can access only a limited amount of data. In Table V we report the size of data used for each update (Size), the number of selected features (FS), the accuracy, the number of communication

Dataset	Size (# obs)	FS (#)	Accuracy (%±C.I.)	R_c (#)	C (%)	N_{OH} (MB)	Cache (MB)
MAV	291	24	96.7±0.4	44	99	16	217
	203	26	96.5±0.3	37	99	13	128
	145	34	97.0±0.3	55	98	20	134
	87	59	97.2±0.3	43	97	15	63
	29	41	97.2±0.4	53	98	19	26
WESAD	$3 \cdot 10^6$	4	93.6±0.8	11	50	0.009	$2 \cdot 10^3$
	$1 \cdot 10^6$	5	93.8±0.5	10	38	0.008	$1 \cdot 10^3$

TABLE V: Performance of FFS varying the data processed during a communication round

rounds upon convergence (R_c), the compression obtainable with FFS (C), the network overhead generated by FFS (N_{OH}), and the size of the cache needed to collect the data before starting the data transmission. Overall, we observe that, for both datasets, decreasing the size of data processed at each round does not affect significantly the number of communication rounds needed by FFS to converge to a solution, which results in limiting the network overhead generated during the process. Specifically, considering a dynamic data collection process as in the MAV-related use case, we see that the network overhead is always i) less than the storage needed to cache the data before starting the transmission and ii) negligible considering the compression achieved (i.e., up to 99%). Interestingly the same holds also for the WESAD scenario. In this case, the network overhead can be considered negligible w.r.t. the size of the data processed ($< 1\text{MB}$) if compared with the compression rate achieved by FFS (up to 50%).

Finally we analyse the FFS performance in presence of *faulty nodes*, i.e., a node experiencing issues in transmitting successfully its updates to the ES. Note that, the causes preventing the updates' transmission might relate to either communication-related (i.e., a noisy channel) or the presence of a power-saving policy regulating the duty cycle of AVs switching off the network interface for a time corresponding to a communication round. Our aim is to assess the robustness of FFS when few nodes cannot contribute to the distributed

learning at each communication round. To this end, we simulate a scenario where, at each communication round, a random number of AVs fail to communicate their updates to the ES. We model the fault of a AV performing a random draw from a Bernoulli distributed random variable, with parameter ρ . At the beginning of the simulation we set ρ and, for each communication round and for each node, we perform a random draw, where 0 means faulty and 1 means non-faulty. This means that the updates of a faulty AV are not considered for the execution of Algorithm 2. In our simulations we consider a fault rate ρ equal to 0.2 and 0.3, meaning that at each round there are, on average, 2 and 3 faulty AVs out of 10, respectively. Such values can be reasonably assumed as upper bounds to evaluate the performance of the system. Higher rates would reveal that the scenario is not reasonably set up to run with any sort of reliability.

In Table VI we report the performance of FFS, for both datasets. For the MAV dataset, although FFS selects $2\times$ and $3.3\times$ more features than the case when all the AVs contribute to the process (see TableIV), the compression rate deteriorates by 1% and 3%, respectively. The quality of the selection is confirmed by the Accuracy that is statistically equivalent to the case without faulty AVs. Regarding WESAD, we notice that for $\rho = 0.2$ FFS performance is equivalent to the case with all non-faulty AVs. Conversely, for $\rho = 0.3$ FFS selects a smaller (i.e., 3 instead of 4) and less informative subset of features, as confirmed by the accuracy degradation. The reason is that the information collected by ES at each round is not enough to select, globally, the most informative features. A final comment is about the network overhead, which can be further reduced, limiting the number of *contributing* AVs during a communication round. In fact, Table VI suggests that there exists a trade-off between accuracy, compression rate and number of *contributing* AVs through which we might optimise both the compression and the resources spent to find it. Moreover, there exists a limit below which saving resources becomes detrimental to the learning process. However, understanding the nature of such a trade-off is left to future works.

Dataset	ρ	FS (#)	Accuracy (% \pm C.I.)	R_c (#)	C (%)
MAV	0.2	48	97.0 \pm 0.4	37	98
	0.3	80	97.2 \pm 0.3	35	96
WESAD	0.2	4	94.5 \pm 0.4	9	50
	0.3	3	67.4 \pm 0.4	7	63

TABLE VI: Performance of FFS varying the percentage non-faulty AVs per communication round

VII. CONCLUSIONS

The increasing development of ADSs can leverage AI to abstract services and applications from the details of fast-flowing low-level data, such as sensor feeds. According to the Edge computing paradigm, a cyber physical system, namely AV, is deputed in collecting data from sensors and perform a

lightweight round of computation, by extracting features from raw data and selecting those that maximise the knowledge on the learning task. Since the data gathering process is performed locally by each AV, the selected features might represent a partial subset of those that characterize the phenomenon and might be inconsistent to learn the model of the underlying process. We tackle this problem, by proposing, for the first time, a FFS algorithm, exploiting a distributed computing paradigm applied to AVs. In FFS, AVs collaborate to come up with the minimal set of features selected from their local datasets, before transmitting their data to the Edge Server. Feature selection is done leveraging on the MI metric and the solution of the optimization problem is achieved through CE method, which allows for approximating a native NP-hard problem into a convex or quasi-convex problem. The aggregation algorithm of the FFS solution is based on a Bayesian approach through which we merge the control information sent by the AVs to the ES. To test the proposed FFS algorithm we presented two different learning tasks, by using real-world datasets: MAV and WESAD. The former was suitable to test FFS with images and inertial measurements, which characterize the position of an AV in the environment. The latter was suitable to characterize time series produced by human state monitoring systems, like ECG, EDA, EMG, etc. Performance evaluation showed that our FFS algorithm allows for achieving up to 99% of compression of the number of features extracted from the datasets at no significant degradation of their informative content. In other words, a learning model trained on the selected features is as accurate as a model trained on the whole feature set, but with a drastically reduced set of transmitted features.

ACKNOWLEDGMENT

This work is partially supported by the MIUR PON project OK-INSAD (GA #ARS01_00917) and by the H2020 projects TEACHING (GA #871385), HumanAI-Net, (GA #952026), MARVEL (GA #957337), and SoBigData++ (GA #871042).

APPENDIX

In this section, we analyze the probability that the distribution \mathbf{p} converges toward the optimal solution \mathbf{p}^* , when the Algorithm 1 is applied in a centralized way. Then, we extend this result for the proposed federated algorithm.

The convergence analysis for the Algorithm 1 is based on the results obtained by the authors in [33]: following the notation in the paper we introduce some preliminaries concepts and definitions. By construction, in the Cross-Entropy procedure the candidate solutions $\{\mathbf{z}_1 \cdots \mathbf{z}_S\}$ generated at iteration t are conditionally independent given the σ -algebra \mathcal{A} at the iteration $t-1$ of all the possible vectors \mathbf{z} , and are identically distributed with distribution $g(\mathbf{z}, \mathbf{p}^{t-1})$.

We define $\mathcal{Z}_t = \{\mathbf{z}_j^\tau \neq \mathbf{z}^* \mid j = 1 \cdots S, \tau = 1 \cdots t\}$ as the set of all the samples generated up to t that do not provide the

optimal solution \mathbf{z}^* . The probability that the optimal solution is not available until t' can be found as in the following:

$$P(\mathbf{z}^{t'} \neq \mathbf{z}^*) = P(\mathcal{Z}_{t'}) = P(\mathcal{Z}_1) \prod_{\tau=2}^{t'} P(\mathcal{Z}_\tau | \mathcal{Z}_{\tau-1}) = P(\mathcal{Z}_1) \prod_{\tau=2}^{t'} (P(\mathbf{z}^\tau \neq \mathbf{z}^* | \mathcal{Z}_{\tau-1}))^S \quad (14)$$

the equation (14) comes from the statistical independence of S identically distributed samples generated by the algorithm at a given iteration. The upper bound for the probability that the optimal solution is not available until τ given that also in $\tau - 1$ wasn't available $P(\mathbf{z}^\tau \neq \mathbf{z}^* | \mathcal{Z}_{\tau-1})$ has been found by the authors in [33] and precisely they shown that:

$$P(\mathbf{z}^\tau \neq \mathbf{z}^* | \mathcal{Z}_{\tau-1}) \leq 1 - P(\mathbf{z}^1 = \mathbf{z}^*) \prod_{i=1}^{\tau-1} (1 - \alpha_i)^m \quad (15)$$

where the $P(\mathbf{z}^1 = \mathbf{z}^*) = \prod_{i=1}^m (p_i^0 \mathcal{I}_{\{z_i^* = 1\}} + (1 - p_i^0) \mathcal{I}_{\{z_i^* = 0\}})$.

Note that due to the definition of \mathcal{Z}_1 its probability is $P(\mathcal{Z}_1) = 1 - P(\mathbf{z}^1 = \mathbf{z}^*)$.

Combining all the results, we obtain

$$P(\mathbf{z}^{t'} \neq \mathbf{z}^*) \leq \left(1 - \prod_{i=1}^m (p_i^0 \mathcal{I}_{\{z_i^* = 1\}} + (1 - p_i^0) \mathcal{I}_{\{z_i^* = 0\}})\right) \prod_{\tau=2}^{t'} \left(1 - \prod_{i=1}^m (p_i^0 \mathcal{I}_{\{z_i^* = 1\}} + (1 - p_i^0) \mathcal{I}_{\{z_i^* = 0\}}) \prod_{j=1}^{\tau-1} (1 - \alpha_j)^m\right)^S \quad (16)$$

The right side of the equation (16) is close to 0 for $t' \rightarrow \infty$, if $\sum_{\tau=1}^{\infty} \prod_{j=1}^{\tau-1} (1 - \alpha_j)^m \rightarrow \infty$, that is, the sequence

of the parameters α_j are generated by the function $\frac{1}{j \cdot m}$, as proven by authors in [34] (section 3.7). Note that, equation (16) can be used to determine numerically a combination of parameter values which yield a desired minimum probability of generating the optimal solution within a time t' .

The results discussed until now prove that the algorithm (1) provides with probability close to 1 the optimal solution when applied in a centralized way. We extend this result for the federated approach, in the following. In our scenario, the nodes draw distinct samples $\mathbf{z}_1 \cdots \mathbf{z}_S$ independently from an identical distribution, as stated in the section V. This means that the node l finds an optimal solution for its \mathbf{z} that differs for m_l entries respect to the optimal solution obtained by the centralized algorithm for $t \rightarrow \infty$. Hence, combining the local distributions into the global one as in equation (9), we need to prove that the local node can receive from the server a federated solution that is close to the solution provided by the centralized scenario, for $t \rightarrow \infty$.

Let's define $\mathcal{Z}_t(m_l) = \{\mathbf{z}_i^\tau \mid z_{j,i}^\tau \neq z_j^*, j \in \{q, \dots, r, \dots, m_l\}, i = 1 \cdots S, \tau = 1 \cdots t\}$ as the set of samples different for m_l entries respect to the optimal solution, which are generated up to time t . As in the case of equation

(14) we can calculate the probability for the event set $\mathcal{Z}_t(m_l)$ for $t = t'$ as in the following:

$$P(\mathcal{Z}_{t'}(m_l)) = P(\mathcal{Z}_1(m_l)) \prod_{\tau=2}^{t'} P(\mathcal{Z}_\tau(m_l) | \mathcal{Z}_{\tau-1}(m_l)) \quad (17)$$

Exploiting again the results provided by the authors in [33], and the statistical independence of the S identically distributed samples generated by the algorithm at a given iteration, the following equation holds for the conditional probability:

$$P(\mathcal{Z}_\tau(m_l) | \mathcal{Z}_{\tau-1}(m_l)) = \left[\binom{m}{m_l} P(z_1 = z^*) \prod_{i=1}^{\tau-1} (1 - \alpha_i)^{m-m_l} \cdot (1 - P(z_1 = z^*) \prod_{i=1}^{\tau-1} (1 - \alpha_i)^{m_l})\right]^S \quad (18)$$

so, the equation (17) becomes:

$$P(\mathcal{Z}_{t'}(m_l)) = P(\mathcal{Z}_1(m_l)) \prod_{\tau=2}^{t'} \left[\binom{m}{m_l} P(z_1 = z^*) \prod_{i=1}^{\tau-1} (1 - \alpha_i)^{m-m_l} \cdot (1 - P(z_1 = z^*) \prod_{i=1}^{\tau-1} (1 - \alpha_i)^{m_l})\right]^S \quad (19)$$

Note that, the result provided in the equation (19) is conditioned to the node l , so the global solution for equation (17) can be evaluate as in the following:

$$P^G(\mathcal{Z}_{t'}(m_l)) = \sum_{l=1}^L P(\mathcal{Z}_{t'}(m_l)) p(l) = \sum_{l=1}^L P(\mathcal{Z}_1(m_l)) \prod_{\tau=2}^{t'} \left[\binom{m}{m_l} P(z_1 = z^*) \prod_{i=1}^{\tau-1} (1 - \alpha_i)^{m-m_l} \cdot (1 - P(z_1 = z^*) \prod_{i=1}^{\tau-1} (1 - \alpha_i)^{m_l})\right]^S p(l) \quad (20)$$

the probability in equation (20) is close to 0, for $t' \rightarrow \infty$, again if $\sum_{\tau=1}^{\infty} \prod_{i=1}^{\tau-1} (1 - \alpha_i)^{m_l} \rightarrow \infty$. Note that, if the sum of products of $(1 - \alpha_i)^{m_l}$ is close to ∞ also the sum of products of $(1 - \alpha_i)^{m-m_l}$ is close to ∞ . The sequences of the α_i parameters guarantee the convergence also in this case. Indeed, the parameters are generated locally by the node, using the function $\frac{1}{m \cdot i}$.

REFERENCES

- [1] Y. Dong, Z. Hu, K. Uchimura, and N. Murayama, "Driver inattention monitoring system for intelligent vehicles: A review," *IEEE transactions on intelligent transportation systems*, vol. 12, no. 2, pp. 596-614, 2010.

- [2] L.-I. Chen, Y. Zhao, P.-f. Ye, J. Zhang, and J.-z. Zou, "Detecting driving stress in physiological signals based on multimodal feature analysis and kernel classifiers," *Expert Systems with Applications*, vol. 85, pp. 279–291, 2017.
- [3] Y. Saeys and P. Inza, I. and Larranaga, "A review of feature selection techniques in bioinformatics," *Bioinformatics Review*, vol. 23, no. 19, pp. 2507–2517, August 2007.
- [4] S. Egea, A. R. Manez, B. Carro, A. Sanchez-Esguevillas, and J. Lloret, "Intelligent iot traffic classification using novel search strategy for fast-based-correlation feature selection in industrial environments," *IEEE Internet of Things Journal*, vol. 5, no. 3, pp. 1616–1624, June 2018.
- [5] G. Brown, "A new perspective for information theoretic feature selection," in *Int. Conf. on Artificial Intelligence and Statistics*, Clearwater Beach, FL, USA, April 2009.
- [6] X. Nguyen, J. Chan, S. Romano, and J. Bailey, "Effective Global Approaches for Mutual Information Based Feature Selection," in *ACM Int. Conf. on Knowledge Discovery and Data Mining*, New York City, NY, USA, August 2014, pp. 1–10.
- [7] D. Rubinstein, R.Y. Kroese, *The Cross-Entropy Method: a Unified Approach to Combinatorial Optimization, Monte-Carlo Simulation, Machine Learning*. Springer, 2004.
- [8] K. Jović, A. and Brkić and N. Bogunović, "A review of feature selection methods with applications," in *IEEE Int. Conf. MIPRO 2015*. IEEE, 2015, pp. 1200–1205.
- [9] B. Venkatesh and J. Anuradha, "A Review of Feature Selection and Its Methods," *CYBERNETICS AND INFORMATION TECHNOLOGIES*, vol. 19, no. 1, pp. 3–26, February 2019.
- [10] F. Chandrashekar, G. Sahin, "A Survey on Feature Selection Methods," *Computers and Electrical Engineering*, vol. 40, no. 1, pp. 16 – 28, 2014.
- [11] L. Miao, J. Niu, "A Survey on Feature Selection," in *Elsevier Int. Conf. on Information Technology , Quantitative Management*, Asan, South Korea, October 2016, pp. 919–926.
- [12] R. Petroccia, P. Cassarà, and K. Pelekanakis, "Optimizing adaptive communications in underwater acoustic networks," in *OCEANS 2019 MTS/IEEE SEATTLE*. IEEE, 2019, pp. 1–7.
- [13] G. F. Anastasi, P. Cassarà, P. Dazzi, A. Gotta, M. Mordacchini, and A. Passarella, "A hybrid cross-entropy cognitive-based algorithm for resource allocation in cloud environments," in *2014 IEEE Eighth International Conference on Self-Adaptive and Self-Organizing Systems*. IEEE, 2014, pp. 11–20.
- [14] F. Guarino, P. Cassarà, S. Longo, M. Cellura, and E. Ferro, "Load match optimisation of a residential building case study: A cross-entropy based electricity storage sizing algorithm," *Applied energy*, vol. 154, pp. 380–391, 2015.
- [15] J. Konečný, B. McMahan, and D. Ramage, "Federated Optimization: Distributed Optimization Beyond the Datacenter," *arXiv Prepr. arXiv1511.03575*, no. 1, pp. 1–5, 2015.
- [16] H. B. McMahan, E. Moore, D. Ramage, S. Hampson, and B. A. y. Arcas, "Communication-Efficient Learning of Deep Networks from Decentralized Data," in *Proc. the 20th International Conf. Artif. Intelligence Stat.*, vol. 54, 2017, pp. 248–50.
- [17] S. Wang, T. Tuor, T. Salonidis, K. K. Leung, C. Makaya, T. He, and K. Chan, "When Edge Meets Learning: Adaptive Control for Resource-Constrained Distributed Machine Learning," *Proc. - IEEE INFOCOM*, vol. 2018-April, pp. 63–71, 2018.
- [18] M. M. Amiri and D. Gunduz, "Machine Learning at the Wireless Edge: Distributed Stochastic Gradient Descent Over-the-Air," no. ML, pp. 1–12, 2019.
- [19] S. P. Karimireddy, S. Kale, M. Mohri, S. J. Reddi, S. U. Stich, and A. T. Suresh, "SCAFFOLD: Stochastic controlled averaging for on-device federated learning," *arXiv*, pp. 1–30, 2019.
- [20] M. Mohri, G. Sivek, and A. T. Suresh, "Agnostic Federated Learning," pp. 1–30, 2019.
- [21] Y. Mao, "Learning from Differentially Private Neural Activations with Edge Computing," *2018 IEEE/ACM Symp. Edge Comput.*, pp. 90–102, 2018.
- [22] V. Mothukuri, R. M. Parizi, S. Pouriyeh, Y. Huang, A. Dehghantanha, and G. Srivastava, "A survey on security and privacy of federated learning," *Future Generation Computer Systems*, vol. 115, pp. 619 – 640, 2021.
- [23] L. Valerio, A. Passarella, and M. Conti, "Hypothesis transfer learning for efficient data computing in smart cities environments," in *International Conference on Smart computing (SMARTCOMP 2016)*, St. Louis, Missouri, IEEE, Ed., 2016.
- [24] —, "A communication efficient distributed learning framework for smart environments," *Pervasive and Mobile Computing*, vol. 41, pp. 46 – 68, 2017.
- [25] X. Ye, H. Li, A. Imakura, and T. Sakurai, "Distributed Collaborative Feature Selection Based on Intermediate Representation," in *In Proc. of Int. Conf. IJCAI 2019*, 2019, pp. 4242–4149.
- [26] P. Schmidt, A. Reiss, R. Duerichen, C. Marberger, and K. Van Laerhoven, "Introducing wesad, a multimodal dataset for wearable stress and affect detection," in *ACM Int. Conf. ICMI 2018*. ACM, 2019, pp. 1–9.
- [27] G. Brown, A. Pocock, M. Zhao, and M. Zheng, "Conditional likelihood maximisation: A unifying framework for information theoretic feature selection," *Springer Journal of Machine Learning Research*, vol. 13, pp. 27–66, 2012.
- [28] R. McEliece, *In The Theory of Information and Coding: A Mathematical Framework for Communication*, ser. Encyclopedia of Mathematics and Its Applications. MA, USA: Addison-Wesley Publishing Company: Reading, 1977, vol. Vol. 3.
- [29] J. Cover, T.M. Thomas, *Elements of Information Theory*. New York, NY, USA: John Wiley and Sons, Inc, 1991.
- [30] A. Chaovalitwongse, I. Androulakis, and P. Pardalos, "Quadratic Integer Programming: Complexity and Equivalent Form," *Springer Encyclopedia of Optimization*, pp. 3153–3159, September 2009.
- [31] P. Chen, C. Huang, C. Lien, and Y. Tsai, "An efficient hardware implementation of hog feature extraction for human detection," *IEEE Transactions on Intelligent Transportation Systems*, vol. 15, no. 2, pp. 656–662, 2014.
- [32] I. Goodfellow, Y. Bengio, and A. Courville, *Deep Learning*. The MIT Press, 2016.
- [33] A. Costa, O. D. Jones, and D. Kroese, "Convergence properties of the cross-entropy method for discrete optimization," *Elsevier Operation Research Letters*, vol. 35, no. 7, pp. 573–580, September 2007.
- [34] K. Knopp, *Infinite Sequences And Series*. Dover Publications Inc., 1956.